

Mapping UHECRs deflections through the turbulent galactic magnetic field with the latest RM data

M. S. Pshirkov^{1,2,3*}, P. G. Tinyakov^{3,4†}, F. R. Urban^{4‡}

¹*Sternberg Astronomical Institute, Lomonosov Moscow State University, Universitetskij prospekt 13, 119992, Moscow, Russia*

²*Pushchino Radio Astronomy Observatory, 142290 Pushchino, Russia*

³*Institute for Nuclear Research of the Russian Academy of Sciences, 117312, Moscow, Russia*

⁴*Université Libre de Bruxelles, Service de Physique Théorique, CP225, 1050, Brussels, Belgium*

ABSTRACT

We study the influence of the random part of the Galactic magnetic field on the propagation of ultra high-energy cosmic rays. Within very mild approximations about the properties of the electron density fluctuations in the Galaxy we are able to derive a clear and direct relation between the observed variance of rotation measures and the predicted cosmic ray deflections. Remarkably, this is obtained bypassing entirely the detailed knowledge of the magnetic properties of the turbulent plasma. Depending on the parameters of the electron density spectrum, we can either directly estimate the expected deflection, or constrain it from above. Thanks to the latest observational data on rotation measures, we build a direction-dependent map of such deflections. We find that over most of the sky the random deflections of 40 EeV protons do not exceed 1 to 2 degrees, and can be as large as 5 degrees close to the Galactic plane.

Key words: ISM: turbulent magnetic fields, cosmic rays

1 INTRODUCTION

Magnetic fields play a crucial role in the propagation of ultra-high energy cosmic rays (UHECRs) — cosmic rays with energies $E > 10^{19}$ eV. If the extragalactic magnetic fields are not too strong (< 1 nG) (Kronberg 1994), the influence of the Galactic Magnetic Field (GMF) should be dominant. Various observations indicate that the magnetic field of our Galaxy contains both regular and turbulent components (see, e.g., Beck (2001, 2008)). If there were only a regular component, a fair knowledge of it would allow one to restore the original positions of the sources from the observed arrival directions of CRs. However, the presence of the turbulent part renders this task very difficult. Unpredictable deflections of CRs in the turbulent fields sum up to random displacements that smear the source image. Thus, the prospects to reconstruct the actual positions of sources depend directly on the parameters of the random part of GMF (hereafter, rGMF).

There is quite a substantial number of studies concerned with the question of UHECR propagation through the GMF (Stanev (1997); Tinyakov & Tkachev (2002); Prouza & Šmída (2003); Takami & Sato (2008);

Giacinti et al. (2010), to name a few). The influence of the random component is rather difficult to estimate and the number of papers on this subject is limited (Harari et al. 2002; Tinyakov & Tkachev 2005; Golup et al. 2009).

The rGMF affects not only the deflections of the CRs, but also contributes to the scatter of the observed values of the Faraday Rotation Measures (RMs) of extra-galactic radio-sources. Moreover, the rGMF enters both quantities in a very similar fashion: they are proportional to the line-of-sight integrals of the perpendicular components of rGMF (in the case of deflections) or the parallel component times the electron density (in the case of RMs). Thus, with some assumptions about the electron density, one can derive predictions/constraints on the random deflections directly from the observed RM variances. The aim of this work is to estimate the UHECR deflections due to rGMF using the recent observational data on the RMs of extragalactic sources, namely the catalogue of RMs obtained by Taylor et al. (2009) from the NRAO VLA Sky Survey (NVSS), further simply referred to as the NVSS RM catalogue.

The underlying logic is straightforward. In general, the variance of RMs over a sufficiently small patch of the sky is composed of the part due to the magnetic fields of our Galaxy (this is the part we are interested in) and another part due to the intergalactic space, the RM intrinsic to the sources, and due to the catalogue errors. The extragalactic contributions can be isolated and subtracted by mak-

* E-mail: pshirkov@prao.ru

† E-mail: petr.tiniakov@ulb.ac.be

‡ E-mail: furban@ulb.ac.be

ing use of their independence of the Galactic latitude. In turn, the Galactic part of the RM variance is a sum of contributions due to rGMF and the variation of the electron density. This relation allows one to either estimate (if the second part can be neglected) or put an upper bound on the part due to rGMF, which translates directly into an estimate/constraint on the UHECR deflections. The result is a position-dependent map of estimates/constraints on the UHECR random deflections. Such a map is important in the UHECR data analysis, for instance, for a more accurate prediction of UHECR flux from a given population of sources.

The paper is organised as follows. Section 2 describes the data. Section 3 presents our method. The results and conclusions are given in section 4. The closing Appendix contains all the technicalities of our method.

2 DATA

In this paper we used the NVSS RM catalogue consisting of 37,543 RM values of extra-galactic sources. We cleaned the catalogue removing the outliers. The algorithm for the cleaning procedure was the following: a circle of 3° radius was circumscribed around every source and the average RM and its variance were calculated for the selected region. If the RM of the source was more than two r.m.s. values away from the average value, the source was marked as “outlier”. In total, 1974 sources were removed after this procedure, leaving 35,569 in the reliable set.

We binned the data using the HEALPix package¹ (Górski et al. 2005) into a map of resolution $N_{\text{side}} = 8$ in the galactic coordinates with the RING pixel ordering. The total number of bins is equal to 768 and the area of each bin is 53 sq. deg. This bin size provided the statistics of ~ 50 RMs in a bin on average. At the same time, it is sufficiently small to neglect the variation of the RM due to the change of the coherent magnetic field across the bin.

Our resolution is thus that of our bins; if there is a very strong and localised regular magnetic field or strong variation of the regular electron density within such region, we would mistakenly interpret it as turbulent. To refine our model one would need to remove the known strong features of the regular galactic field and electron density. It would be also possible to exclude bins whose RM, compared with neighbouring bins, exceeds a given threshold. However this introduces one more parameter in order to control the acceptance of the different bins. We opt instead for a minor mistake in the interpretation of the result, but for a very simple logic, and also mathematical trackability.

3 METHOD

3.1 Intrinsic variance

As already mentioned, the observed RM variance $\langle RM^2 \rangle \equiv \sigma$ consists of two main parts²: the variance σ_{ISM} due to the

interstellar medium (ISM) we are interested in, and the variance σ_{QSO} that is caused by other factors, including those intrinsic to the sources. We estimated the variance σ_{QSO} using the data itself by making use of the fact that the latter part should be independent of direction, while the latitude (b) dependence of σ_{ISM} should look like $1/\sin b$ due to purely geometrical reasons. As we show below, a simple toy model of identical cells of turbulent field up to some height z_{thr} predicts this dependence (see section 3.3).

Our method for separating the two variances had previously been introduced in (Schnitzeler 2010). We have here slightly adapted this method for our purposes, and recalculated these variances anew: our results agree nicely with those obtained by Schnitzeler.

In order to estimate σ_{QSO} we performed the following calculations. In the Northern hemisphere we fitted the observed $\sigma(b)$ for 36 uniformly spaced values $l = 0^\circ, 10^\circ, \dots, 350^\circ$ with the function $f(b) = (A^2/\sin^2 b + \sigma_{\text{QSO}}^2)^{1/2}$ treating A and σ_{QSO} as free parameters. The bins with $b < 10^\circ$ were excluded. We then calculated the mean and the r.m.s. values of the resulting 36 values of σ_{QSO} .

The same procedure was independently performed for the Southern hemisphere. In both cases we obtained very close numbers: $\sigma_{\text{QSO}} = (12 \pm 3) \text{ rad m}^{-2}$. Thus, for the following calculations we adopted $\sigma_{\text{QSO}} = 12 \text{ rad m}^{-2}$. This value is largely dominated by the intrinsic errors of the NVSS RM catalogue $\sigma_{\text{NVSS}} = 10.4 \pm 0.4 \text{ rad m}^{-2}$.

Making use of this result, we estimated σ_{ISM} for each bin as follows:

$$\sigma_{\text{ISM}} = \sqrt{\sigma^2 - \sigma_{\text{QSO}}^2}, \quad \sigma > 12 \text{ rad m}^{-2}. \quad (1)$$

Both σ and σ_{QSO} are determined with errors. The error of σ_{QSO} is $\delta\sigma_{\text{QSO}} = 3 \text{ rad m}^{-2}$ as explained above. The error of σ depends on the number n of sources in the bin and equals $\delta\sigma = \sigma/\sqrt{2n}$. This implies the error $\delta\sigma_{\text{ISM}}$ in determination of σ_{ISM} ,

$$\delta\sigma_{\text{ISM}} = \sqrt{\delta\sigma_{\text{QSO}}^2 + \delta\sigma^2}.$$

In those bins where the value of σ_{ISM} inferred from eq. (1) was smaller than $\delta\sigma_{\text{ISM}}$ we have set $\sigma_{\text{ISM}} = \delta\sigma_{\text{ISM}}$. This includes 29 bins with $\sigma < \sigma_{\text{QSO}}$.

Finally, we discarded the bins with the number of sources less than 10 (130 bins total) located in the “blind spot” of the NVSS survey (declination $< -40^\circ$) and its immediate vicinity.

3.2 Rotation measures vs. deflections

When propagating through a magnetised plasma, the polarisation plane of a linearly polarised electromagnetic wave of wavelength λ rotates by the angle $\Delta\psi$ proportional to the square of the wavelength,

$$\Delta\psi = RM \cdot \lambda^2, \quad (2)$$

where the coefficient RM, the rotation measure, can be expressed in terms of the properties of the interstellar medium (ISM) and permeating magnetic fields. Since the same magnetic field also deflects UHECRs, both processes can be de-

¹ <http://healpix.jpl.nasa.gov>

² In this subsection *only* we denote $\langle RM^2 \rangle \equiv \sigma$ so as to not clutter notation.

scribed by similar expressions, functions of the direction \hat{r} :

$$RM(\hat{r}) = c_1 \int_0^D dz n B_{\parallel}, \quad (3)$$

$$\vartheta_i(\hat{r}) = c_2 \int_0^D dz \epsilon_{ij} B_j, \quad (4)$$

where n is the electron density, B_{\parallel} and B_i , $i = (1, 2)$ are the components of the magnetic field parallel and perpendicular to the direction \hat{l} , respectively, D is the distance to the source, and the normalisation constants are $c_1 = 0.81 \text{ rad cm}^3 / (\text{m}^2 \text{ pc } \mu\text{G}) \approx 2.7 \times 10^{-23} \text{ rad}/\mu\text{G}$, $c_2 = Ze / (E \mu\text{G})$, Z and E being the UHECR charge and energy, respectively. For our further estimates we assume that UHECRs are protons ($Z = 1$) and have energy equal to 40 EeV, thence $c_2 = 7.5 \times 10^{-24} \text{ rad}/(\mu\text{G cm})$. For further reference, we also give the ratio

$$\frac{c_2}{c_1} = 0.28 \text{ cm}^{-1}. \quad (5)$$

These estimates could be easily rescaled for any given composition and energy of UHECRs.

The presence of the random component induces variances both on the observed RMs and on the deflections of UHECRs. Although both mean deflections and mean RMs are by definition zero for a random field, their r.m.s. are not. The variations in RM are caused by fluctuations both in the magnetic field and the electron density, whereas variations in ϑ are produced by magnetic fields fluctuations alone. This makes the link between the two rather contrived in general.

Let us separate the regular and random components as $n = \langle n \rangle + \delta n$ and $B_i = \langle B \rangle_i + \delta B_i$, and similarly for $B_3 \equiv B_{\parallel}$ — all these quantities are taken to not depend on the absolute vertical distance to the observer, see the Appendix. Conversely RM and ϑ_i already refer to the (square roots of) their variances, and there will be no need to prepend a “ δ ” to them. With this notation, and within very mild approximations we can spell out the connection between $\langle RM^2 \rangle$ and $\langle \vartheta^2 \rangle \equiv \sum \langle \vartheta_i \vartheta_i \rangle$.

Schematically, for some positive coefficients α and β of appropriate units, we show in the Appendix that we can write:

$$\langle RM^2 \rangle = c_1^2 \langle n \rangle^2 \langle \mathcal{I}^2(\delta B) \rangle + \alpha \langle \mathcal{I}^2(\delta B) \rangle + \beta, \quad (6)$$

$$\langle \vartheta^2 \rangle = c_2^2 \langle \mathcal{I}^2(\delta B) \rangle, \quad (7)$$

cf. (3) and (4). We also have used the shorthand notation $\mathcal{I}(\star) \equiv \int dz \star$. In eq. (6), the first term comes from the variation δB alone, the second depends on both δB and δn (the latter enters through the coefficient α), while the third depends only on δn . The coefficients α and β are both, therefore, proportional to $\langle \delta n^2 \rangle$.

There are several parameters which enter the game at this stage, and impact the values of the coefficients α and β . Before dwelling upon these details, we see that there are two options. If the properties of δn are such that both α and β are small, the corresponding terms can be neglected. Then the magnetic fluctuations factorise out altogether and we immediately infer

$$\langle \vartheta^2 \rangle = \frac{c_2^2}{c_1^2 \langle n \rangle^2} \langle RM^2 \rangle. \quad (8)$$

In this case we link directly (within the limits of the regular electron density model) rotation measures with deflections.

In the opposite case of non-negligible α and β , there are additional, positive by construction, contributions to $\langle RM^2 \rangle$. Then, the contribution of the magnetic field variance $\langle \delta B^2 \rangle$ alone to the RM one would be an overestimation, and (8) remains valid although only as an upper limit. We discuss the goodness of this upper bound below, but first, in Sec. 3.3 we develop a simplified toy model which provides an additional intuitive argument to understand the physics behind (8).

Before moving further, we need to mention a potential caveat of our approach. Imagine that the regular magnetic field is strong enough as to deviate cosmic rays away from their paths by an angle which is significantly larger than the size of our bins. If this is the case, then we are comparing two different lines of sight, the deflected cosmic ray, and polarised radio waves, which do not belong to the same bin. We would be then inferring some properties of the former from the latter, but the two would not be causally connected, and the information extracted not meaningful.

Throughout our analysis we have in mind proton primaries, whose deflections at the energies of interest, as we checked, are significantly smaller than the size of our bins; hence, the complete algorithm works smoothly. The limit of our simplification is of course in this assumption.

For heavier composition one needs to make sure that the UHECRs trajectories are not deflected too much. Notice that in any case it would still be possible to apply our method, but first the UHECRs paths through the regular magnetic field need to be reconstructed, so as to assign each source to its appropriate bin. This however introduces a significant complication and model-dependence (on the regular field).

One important reason we decided to focus on the simplest case for, is that all equations are derivable in a streamlined and logic way, where all the key parameters show up in the final expressions. This makes it very versatile in understanding the physics, and in giving reasonable estimates for a wide range of parameters which to date are still very uncertain. With the assumptions clearly spelt out, and the simple results at hand, it is easy to generalise to more complicated models once better data become available.

In this paper we have chosen to work with the model of Pshirkov et al. (2011). We have explicitly checked that, for proton primaries, the perpendicular coherent deflections caused by the regular magnetic field do not cause the events to jump across to the wrong bin.

Given this key assumption we can perform our analysis in the simple way as we have outlined in this section. It is important to notice that, *a posteriori*, we can also check that the random deflections we finally obtain do not exceed the size of our bins, which makes our assumption self-consistent.

3.3 A toy random walk model

The variance of the deflections experienced by UHECRs could be estimated within a simple cell model: the random field with given strength B_r is chopped into identical cells with size l_{cell} ; in each cell the magnetic field is uniform and has some random orientation. The electron density n is assumed to be constant. RMs would then perform a random walk along the line of sight, which we can put in formulas

as

$$RM = k_1 RM_0 \sqrt{N}, \quad (9)$$

where k_1 is a numerical coefficient, N is the total number of cells along the line of sight, RM_0 is the average contribution of the elementary cell — one can think of this as (3) with $\int dz \rightarrow l_{\text{cell}}$.

The deflections in this model are described by a very similar formula:

$$\vartheta = k_2 \vartheta_0 \sqrt{N}, \quad (10)$$

where k_2 is another coefficient, and ϑ_0 is the deflection in the elementary cell (once again, take (4) and replace $\int dz \rightarrow l_{\text{cell}}$).

The exact value of the coefficients k_1, k_2 were calculated numerically. First we simulated the random walk for the RM accumulation. Taking into account that only the parallel component of the magnetic field contributes proportionally to $\cos \phi_i$, where ϕ_i is the angle between the random direction of the magnetic field and the direction of the line of sight, then, k_1 reads

$$k_1 = \frac{\left| \sum_{i=1}^N \cos \phi_i \right|}{\sqrt{N}}, \quad (11)$$

where ϕ_i is a random variable in $[0, \pi]$ range. The number of steps N was taken equal to 100,000 and we averaged over 10,000 realisations, obtaining finally

$$k_1 = 0.56.$$

The coefficient k_2 could be obtained in the very same fashion, but now there is a two-dimensional random walk process and also it is the orthogonal component of the magnetic field that should be taken into account. One finds

$$k_2 = \frac{\sqrt{\left(\sum_{i=1}^N \sin \phi_i \cos \psi_i \right)^2 + \left(\sum_{i=1}^N \sin \phi_i \sin \psi_i \right)^2}}{\sqrt{N}}, \quad (12)$$

where ϕ_i is again a random variable in the $[0, \pi]$ range, whereas ψ_i has domain $[0, 2\pi]$. We obtain

$$k_2 = 0.63.$$

Putting everything together, the relation between the RM and the deflection along the same path is

$$\vartheta \approx 0.31 \text{ cm}^{-1} \frac{k_2}{k_1} \frac{RM}{\langle n \rangle} \approx 0.35 \text{ cm}^{-1} \frac{RM}{\langle n \rangle}. \quad (13)$$

This result is to be compared with the more accurate expression (8) where, for $E = 40$ EeV and $Z = 1$ (protons), the coefficient turns out to be $c_2/c_1 \approx 0.28 \text{ cm}^{-1}$, cf. eq. (5). The two expressions are therefore in close agreement, the more so in light of the observational and theoretical errors we are faced with: the toy model correctly distillates the physics, and provides clear and intuitive insight for our idea.

3.4 General case

We turn now to discussing the parameters which enter in α and β , and the interpretation of (8). For concreteness we focus on the simplest, and most corroborated by the data, scenario (Armstrong et al. 1995; Haverkorn et al. 2008). We

thus employ a Kolmogorov electron density spectrum to obtain

$$\begin{aligned} \langle RM^2 \rangle &\simeq c_1^2 \langle n \rangle^2 \langle \mathcal{I}^2(\delta B) \rangle \\ &+ c_1^2 \left[3.1 C_n^2 l_0^{2/3} \langle \mathcal{I}^2(\delta B) \rangle + 1.1 C_n^2 D l_0^{5/3} \langle B \rangle^2 \right], \end{aligned} \quad (14)$$

where C_n^2 is the amplitude of the Kolmogorov spectrum, and the momentum IR cutoff is given by $q_0 = 2\pi/l_0$, with l_0 the largest scale of turbulence (with a given spectral index); finally, D is the path length along which the electron density turbulence extends (and, as we expect for the magnetic field one, it will roughly follow a $1/\sin(b)$ distribution). The details of the calculation are given in the Appendix.

As previously mentioned, there are two possibilities. If the magnetic field variance dominates this expression, then there is a simple direct relation $\langle RM^2 \rangle \propto \langle \mathcal{I}(\delta B)^2 \rangle$. The second option is that the $\langle B \rangle^2$ term wins, in which case the measured RMs would be due to a combination of fluctuations in the electron density and the magnetic field, which we can not disentangle; the contribution of the magnetic field variance $\langle \delta B^2 \rangle$ to the UHECR deflections would then be smaller than in eq. (8), so the latter would be an over-estimation and would, therefore, provide one with an upper bound on the deflections.

We can also turn this argument around. Assume a given set of parameters which describe the electron density, its fluctuations and the average magnetic field. We can ask which would be the contribution of the last term (independent of the unknown $\langle \delta B^2 \rangle$) to the measured RM. If this is actually larger than what is observed, the conclusion is that the set of parameters used is not consistent with the RM data. Still, eq. (8) gives a valid upper bound for a given electron density.

Consider the parameters that enter eq. (14). First, we fix the value of the path length D that should be inserted into our calculations. The variances get contributions only in regions where considerable magnetic fields and electron density are present. Both quantities are usually assumed to decay very rapidly with the height h above the Galactic plane: like $\text{sech}^2(h/d)$ (Cordes & Lazio 2002); or $\exp(-h/d)$ (Gaensler et al. 2008), albeit with possibly somewhat different vertical scales d . To describe the electron density distribution we use the NE2001 model (Cordes & Lazio 2002) modified with an increased vertical scale ($n(h=0) \approx 0.014 \text{ cm}^{-3}$, $d = 1.8 \text{ kpc}$), which is implied by recent observations (Pshirkov et al. 2011) (see also (Gaensler et al. 2008); in (Savage & Wakker 2009; Taylor & Cordes 1993) instead lower values for d were preferred: it is immediate to rescale all our results for any of these options, see below). We adopt this vertical scale and cut the integrals at the value $D = d/\sin(b)$. Notice that since all three terms in eq. (14) are roughly proportional to D , their relative magnitude does not depend strongly on the adopted value. Finally, we also assume that the vertical scale of the turbulent part of the GMF does not exceed $\sim 2 \text{ kpc}$, i.e., magnetic field and electron density regions are largely spatially coincident (see Sec. 4 for more details).

Moreover, notice that we do not treat explicitly the h -dependence of the average $\langle n \rangle$ itself, which would also behave as $\text{sech}^2(h/d)$ or $\exp(-h/d)$, although we do keep the dependence with direction. In doing so we are making an approximation equivalent to substituting the steep suppres-

sion with a sharper step function localised at $h = d$, with the advantage that we can calculate everything analytically. This boosts the deflection we obtain by at most around 30% (this approximate value is obtained by comparing the integrals of a simple step function against the actual behaviour, however ignoring any h/d -dependence.), which is not large an error in view of the accuracies we have at hand.

Recall also our discussion at the end of Sec. 2: our results are interpreted as upper limits on the turbulent deflections. If there are isolated, strong variations of the regular electron density field we would interpret them as coming from random fields: this does not impair the final result, and in principle such features can be removed to tighten the constraint we infer.

The mean magnetic field $\langle B \rangle$ entering eq. (14) can be inferred from the existing models of the coherent Galactic field. We adopt $\langle B \rangle$ estimated from the model (Pshirkov et al. 2011); alternatively, one could use, e.g., the model (Jansson & Farrar 2012).

The statistical properties of δn are not very well known. The analyses of Armstrong et al. (1995) and Haverkorn et al. (2008) have obtained $C_n^2 = 10^{-3} m^{-20/3}$ and an IR scale of $l_0 = 100$ pc (at large b). Again, these values are expected to change with direction because of the morphology of the galaxy, but the data are uncertain and we will rely on the simplifying approximation that these parameters remain the same across the sky. These are our fiducial parameters, which we employ in drawing the deflection map. With these values, for a typical average magnetic field of $1 \mu\text{G}$ and $b = 90^\circ$, the third term in eq. (14) amounts to about 17 rad/m^2 , which overshoots the observed RM in a large part of the sky, although not by much. We have therefore a situation described above when the parameters are not quite consistent with the observed RMs. If this inconsistency is attributed to the numerical uncertainties, one concludes that the third term in eq. (14) dominates and thus eq. (8) is an overestimate.

We have also tried different parameters set, besides the blueprint values mentioned above. The first possible modification is to rescale the vertical scale of electron density to 1.3 kpc instead of 1.8 kpc, as suggested by Schnitzeler (2012). The main effect in this case is that $\langle n \rangle$ is somewhat increased, which implies that the resulting deflections will be smaller. The physics does not change however, and the same qualitative conclusions can be drawn. The displacement angles are diminished by at most around 20% in some parts of the sky, which is not significant within our approximations.

Then, so far we have always assumed exact Kolmogorov turbulence all the way up to the IR cutoff l_0 of 100 pc. Nevertheless, the observational scenario is far from being clear, and there is the possibility that the spectrum actually flattens at larger scales; there are indications of this flattening for the *turbulent magnetic field* (Regis 2011), although it is uncertain what the link between the two is at large scales. Within our formalism it is immediate to estimate its effects: as a concrete case, taking the spectral index $\alpha = 3$ from 1 pc to 100 pc suppresses the contribution of the third term in eq. (14) to the total RMs by a factor of $100^{-1/3}$, bringing it down to about 4 rad/m^2 , which is below the intrinsic threshold we adopt. In this case (8) becomes a much better estimation of the deflections: if we ask that the third term in eq. (14) contributes at most to 20% of the observed

RM, then any RM above about 20 rad/m^2 would provide a direct connection to $\langle \vartheta^2 \rangle$ (within our approximations). Let us emphasise however that we have stuck to the baseline parameters for the map, and ensuing discussion.

The last comment is on the second term in eq. (14). This term has the same dependence on $\langle \delta B^2 \rangle$ as the first one, so the two can in principle be combined together, which would change (make smaller) the coefficient in eq. (8). Although this would strengthen the constraints on the deflections for a given value of RM, it would also make them dependent on the (poorly known) properties of the electron density fluctuations. For this reason we do not include this term in our final constraints. Using again the fiducial values of Armstrong et al. (1995) and Haverkorn et al. (2008) we find $1.76 C_n l_0^{1/3} \sim 0.080 \text{ cm}^{-3}$, which is larger than the model average of NE2001; the latter is, $\langle n \rangle \approx 0.012 \text{ cm}^{-3}$. Using instead the spectral index $\alpha = 3$ from 1 pc to 100 pc suppresses this contribution down to 0.017 cm^{-3} , thereby bringing it around the mean value of NE2001.

To summarise, within present uncertainties of the parameters of the electron density fluctuations, both third and second terms in eq. (14) can be sizeable, but their values cannot be reliably determined at present. Because of these uncertainties, we base our constraints on eq. (8) which we treat as an upper bound on deflections $\langle \vartheta^2 \rangle$.

4 RESULTS AND CONCLUSIONS

As explained above, eq. (8) provides one with an upper bound (or an estimate, if the contributions of the fluctuations of the electron density can be neglected) on the UHECR deflections $\langle \vartheta^2 \rangle$ in the random component of the Galactic magnetic field. These deflections can be translated into the experimentally observable displacements $\langle \Theta^2 \rangle$ of the UHECR arrival directions at the Earth with respect to the direction to the true position of the source. The relation between the two quantities is (Harari et al. 2002):

$$\langle \Theta^2 \rangle = \langle \vartheta^2 \rangle / 3. \quad (15)$$

In Fig. 1 we show the map of deflections $\sqrt{\langle \Theta^2 \rangle}$ of protons with energy $E = 4 \times 10^{19}$ eV due to the random component of the GMF calculated according to eq. (8) where we have used the value $c_2/c_1 = 0.28 \text{ cm}^{-1}$. This map should be considered an upper bound, which may turn into an estimate if the contribution of the electron density fluctuations will be shown to be small in the future. The displacements $\sqrt{\langle \Theta^2 \rangle}$ are bound to 1 to 2 degrees for the majority of directions, although closer to the galactic plane the bounds are relaxed to $\sim 5^\circ$. This map is the main result of our paper.

One can see from Fig. 1 that the limit on deflections does not depend on the Galactic longitude in any regular way. In particular, the direction towards the Galactic centre does not look any special. On the contrary, there is a regular dependence on the Galactic latitude b . This dependence is fitted well with the phenomenological function $A/(\sin^2(b) + B)$, with the constants $A = 0.5$, $B = 0.13$, although the fluctuations are large. For the purpose of describing the upper bound, the constraints of Fig. 1 can be majorated by the analytic function

$$\sqrt{\langle \Theta^2 \rangle} < \frac{1^\circ}{\sin^2(b) + 0.15} \quad (16)$$

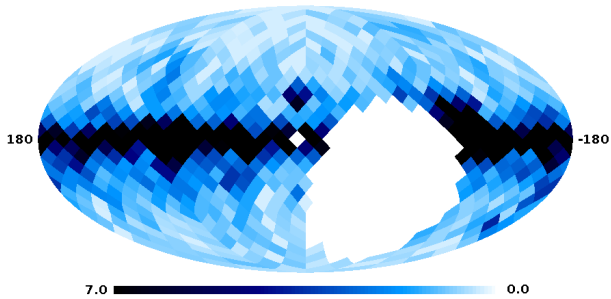


Figure 1. The map of displacements $\sqrt{\langle \Theta^2 \rangle}$, of protons with energy $E = 4 \times 10^{19}$ eV due to the random component of the GMF as follows from eq. (8). The map is in Galactic coordinates and the displacements are in degrees. This map should be considered as an upper bound and may turn to an estimate if the contribution of the electron density fluctuations are small, as explained in the text.

everywhere except several bins.

The results obtained in the paper are in good agreement with results of Tinyakov & Tkachev (2005). In the latter paper the deflections in the turbulent field were derived using properties of the rGMF inferred from few observations coming from different sets of data. It was shown that for 40 EeV protons such deflections are small, not exceeding 1.5° for the better part of the sky. The most important difference with that work, where one was obliged to use a specific model (i.e., spectrum) for the rGMF fluctuations to draw some quantitative conclusion, is that here we were able to place robust upper limits from a single, thereby consistent, set of data.

A word of warning is in order. While the constraints shown in Fig. 1 are conservative in the sense that we have treated all the uncertainties in a way that increases the deflections (and thus weakens the constraints), they only apply to the contribution of the region of ± 2 kpc around the Galactic disk where the electron density is large and constrained by observations. One cannot exclude, by the arguments presented in the paper, that there might exist more extended regions around the Galaxy that carry small electron density and substantial magnetic fields such that their contributions to the RMs are small, but the contribution to deflections of UHECRs is larger than in eq. (8) like in the model of Ahn et al. (1999). Constraints on such models require a different approach, which we leave for future study.

One needs to bear in mind that one technical limitation of our method is related to our resolution; for instance, the dark spot just to the left and north of the Galactic Centre is caused by the HII region surrounding the star Zeta Ophiuchi (Harvey-Smith et al. 2011), and is a large-scale field that shows structure on scales smaller than the cell size we use. This would naïvely incorrectly be counted as a particularly strong random fluctuation. To refine the map all such known strong features should be removed. However this introduces a high degree of uncertainty and does not add much to the main conclusions; the interpretation of the map as an upper bound is anyhow not compromised.

To conclude, there are three main lessons which we have learnt from this analysis. Firstly, the deflections across the sky do not exhibit strong feature in Galactic longitude; it

is not possible to tell the Galactic centre apart from the anticentre, for example. Secondly, there is instead a clear regularity in Galactic longitude; we have provided a simple phenomenological fit which is of direct implementation for UHECRs anisotropy studies. Thirdly, the overall magnitude, for high energy proton primaries of $E \gtrsim 40$ EeV, does not exceed 5° ; in fact, it is typically quite smaller over most of the sky — especially away from the plane.

The use of RM data to constrain UHECRs deflections has thus revealed to be intuitive, solid, efficient, and effective, within the approximations of the method; a method which is easily and readily generalised and improved, accounting for any new data for modelling electron density and galactic magnetic field.

ACKNOWLEDGEMENTS

This research has made use of NASA’s Astrophysics Data System. Some of the results in this paper have been derived using the HEALPix (K. M. Górski et al., 2005, ApJ, 622, p759) package. The authors thank M. Haverkorn for useful correspondence, S. Troitsky for comments on the manuscript, and D. Schnitzler for constructive remarks. FU wishes to thank the Institute for Theoretical Astrophysics of Oslo, where part of this work was completed. The work of MP is supported by RFBR Grants No. 12-02-31776 mol.a, No. 13-02-00184a, No. 13-02-01311a, No. 13-02-01293a, by the Grant of the President of Russian Federation MK-2138.2013.2 and by the Dynasty Foundation. FU and PT are supported by IISN project No. 4.4502.13 and Belgian Science Policy under IAP VII/37.

APPENDIX

We describe here in details the formal steps that lead to the relation (8) between the variances of RM and deflections.

Definitions

The two quantities we want to calculate are

$$RM(\hat{r}) = c_1 \int_0^D dz n B_{\parallel},$$

$$\vartheta_i(\hat{r}) = c_2 \int_0^D dz \epsilon_{ij} B_j;$$

more specifically, we need the variances of these quantities. In principle, both the random variations in electron density and magnetic field are present. Thus, we split $n = \langle n \rangle + \delta n$ and $B_i = \langle B \rangle_i + \delta B_i$, where $i = (1, 2)$ denotes the two components perpendicular to the line of sight, and similarly for $B_3 \equiv B_{\parallel}$.

In what follows we approximate the actual distance (from the observer) dependence of such quantities is that of a pure step function. This is certainly a good approximation as it captures its key feature: a sharp drop beyond a given distance D . Indeed, we do expect that both the electron density and magnetic field (regular components and fluctuations alike) follow the smoothed distribution of ionised gas in the galaxy, which is typically coded as $\text{sech}^2(x)$ (Taylor & Cordes 1993; Cordes & Lazio 2002)

or $\exp(-x)$ (Lyne et al. 1985; Gaensler et al. 2008) (x is the vertical distance from the observer normalised to d); both these functions do not vary exaggeratedly up to $x \sim 1$ and rapidly decay beyond that point — the mistake we are making in treating these as step functions is of, at most, around 30%, which is well below our other uncertainties. We are therefore allowed to average, along the line of sight, the regular components $\langle n \rangle$ and $\langle B \rangle$ within the integrals and bring them outside. This also implies that the spectra of fluctuations will not depend on the absolute position, but only on the scale.

Thus, we define

$$I_{ij} = \langle \delta B_i(\bar{r}_0) \delta B_j(\bar{r}_0 + \bar{r}) \rangle \\ = \int d^3 q e^{-i\bar{r}\bar{q}} \frac{P_B(q)}{2q^3} \left(\vartheta_{ij} - \frac{q_i q_j}{q^2} \right),$$

where we used the Fourier transform

$$\delta B_i(\bar{r}) = \int d^3 q e^{i\bar{r}\bar{q}} \delta B_i(\bar{q}),$$

and the spectrum is defined as

$$\langle \delta B_i(\bar{q}) \delta B_j^*(\bar{p}) \rangle = \frac{P_B(q)}{2q^3} \left(\vartheta_{ij} - \frac{q_i q_j}{q^2} \right) \delta^3(\bar{q} - \bar{p}).$$

Similar definitions apply to δn :

$$\delta n(\bar{r}) = \int d^3 q e^{i\bar{r}\bar{q}} \delta n(\bar{q}),$$

and

$$\langle \delta n(\bar{q}) \delta n^*(\bar{p}) \rangle = \frac{P_n(q)}{q^3} \delta^3(\bar{q} - \bar{p}).$$

Notice that $I_{ij} \propto \vartheta_{ij}$ since otherwise it is zero (parity). Writing the integrals explicitly, they all reduce to the prototype

$$I_i = \int d \cos \vartheta d\vartheta dq^2 e^{-i r q \cos \vartheta} \frac{P_B(q)}{2q^3} \left(1 - \frac{q_i^2}{q^2} \right),$$

where we call z the line of sight axis. The angular integrals can be solved to give

$$I_1 = I_2 = 2\pi \int \frac{dq}{q} P_B(q) \left(\frac{\sin qr}{qr} + \frac{\cos qr}{q^2 r^2} - \frac{\sin qr}{q^3 r^3} \right), \\ I_3 = I_{\parallel} = 4\pi \int \frac{dq}{q} P_B(q) \left(\frac{\cos qr}{q^2 r^2} - \frac{\sin qr}{q^3 r^3} \right).$$

Our assumptions on the properties of these fluctuations with vertical distance amount to assuming that the spectra we have hitherto defined do not depend on such quantity, but only on the (modulus of the) correlation length r .

The next step is to integrate along the line of sight:

$$\langle \vartheta_i \vartheta_i \rangle = c_2^2 \int_0^D dz dz' \epsilon_{ij} \epsilon_{ik} \langle \delta B_j(z) \delta B_k(z') \rangle \\ = 2c_2^2 \int_0^D du \int_0^u dr (I_1 + I_2) \\ = 4\pi c_2^2 \int \frac{dq}{q} P_B(q) \left(q D Si(qD) + \cos qD - \frac{\sin qD}{qD} \right);$$

here we have defined $r = z' - z$ and $u = z' + z$, and $Si(x)$ is the sine-integral function.

A very similar result can be obtained for the RM. The

full expression for the variance of RM , containing all pieces, reads

$$\langle RM^2 \rangle = c_1^2 \int_0^D dz dz' \left[\langle n \rangle^2 \langle \delta B_{\parallel}(z) \delta B_{\parallel}(z') \rangle \right. \\ \left. + \langle \delta n(z) \delta n(z') \rangle \langle B_{\parallel} \rangle^2 + \langle (\delta B_{\parallel} \delta n)(z) (\delta B_{\parallel} \delta n)(z') \rangle \right]. \quad (17)$$

where the first term, $\langle \delta B_{\parallel}^2 \rangle$, is the contribution of rGMF proper, the second one, $\langle \delta n^2 \rangle$, is that of the electron density fluctuations alone, and the last one represents the convolved variations.

Notice that in this scheme we need to compare two quantities whose lines of sight are “compatible”, which in our language means they must reside in the same bin. If the regular magnetic field is strong enough as to deviate cosmic rays away from their paths by an angle which is significantly larger than the size of our bins, then the two different trajectories, the deflected cosmic ray, and polarised radio waves, are not causally connected, and our method does not apply. There is no conceptual obstacle to taking this effect fully into account, by mapping the deflected UHECRs paths on the sphere through the regular field; these reconstructed lines of sight can then be employed for the analysis. We do not do so, for we work with proton primaries whose deflections are small. More details are given in the main text.

A simplified result

If the variance on the electron density fluctuations is small, then the only significant term left in the lengthy expression (17) is the first, leading to

$$\langle RM^2 \rangle = c_1^2 \langle n \rangle^2 \int_0^D dz dz' \langle \delta B_{\parallel}(z) \delta B_{\parallel}(z') \rangle \\ = 4\pi c_1^2 \int \frac{dq}{q} P_B(q) \left(q D Si(qD) + \cos qD - 2 + \frac{\sin qD}{qD} \right).$$

To further simplify this expression, one can expand for large distances and small coherence length $qD \gg 1$ to obtain

$$\langle \vartheta^2 \rangle = 4\pi c_2^2 \int \frac{dq}{q^3} P_B(q) \left(\frac{\pi}{2} qD + \dots \right), \\ \langle RM^2 \rangle = 4\pi c_1^2 \langle n \rangle^2 \int \frac{dq}{q^3} P_B(q) \left(\frac{\pi}{2} qD + \dots \right).$$

This demonstrates now the two quantities are, in first approximation, directly related, and one can infer the deflections caused to the UHECRs *without knowing anything about the spectrum of the magnetic field*. Of course this result makes use of the assumption that there are not any large electron density fluctuations, the goodness of which we discuss in the next section.

The convolution

We now want to determine the contribution of the convolution

$$\begin{aligned} & \langle (\delta B_{\parallel} \delta n)(z) (\delta B_{\parallel} \delta n)(z') \rangle \\ &= \int d^3 k d^3 k' e^{-i\vec{k}\vec{z} - i\vec{k}'\vec{z}'} \langle (\delta B_{\parallel} \delta n)(\vec{k}) (\delta B_{\parallel} \delta n)(\vec{k}') \rangle \\ &= \int d^3 p d^3 q e^{-i(\vec{q}+\vec{p})(\vec{z}'-\vec{z})} \frac{P_n(p)}{p^3} \frac{P_B(q)}{2q^3} \left(\vartheta_{\parallel} - \frac{q_{\parallel}^2}{q^2} \right) \\ &= (4\pi)^2 \int \frac{dp}{p} \frac{dq}{q} P_n(p) P_B(q) \frac{\sin pr}{pr} \left(\frac{\sin qr}{q^3 r^3} - \frac{\cos qr}{q^2 r^2} \right). \end{aligned}$$

This has to be integrated twice over z and z' , or r and u as usual. One reasonable assumption, which simplifies greatly the (euphemistically) unwieldy result, is that the integral is going to be dominated by the IR cutoffs, since observations tell us that the spectra are almost certainly red. The integral can then be split in two, for $p \ll q$ and $p \gg q$ depending on which IR cutoff is the most important one. The result can (now) be expanded for large qD if this is the dominant cutoff, or, conversely for large pD to find

$$\langle RM^2 \rangle \subset (2\pi)^3 c_1^2 \int \frac{dp}{p} \frac{dq}{q} P_n(p) P_B(q) \begin{cases} \frac{2}{3} \frac{D}{q} & p \ll q, \\ \frac{D}{p} & p \gg q. \end{cases}$$

Compare these with the integrated $\langle \delta n^2 \rangle$ and $\langle \delta B^2 \rangle$ in the same limit of large pD and qD — recall that $\mathcal{I}(\star) \equiv \int dz \star$:

$$\begin{aligned} \langle \mathcal{I}(\delta n)^2 \rangle &= -4\pi^2 \int \frac{dp}{p} P_n(p) \frac{D}{p}, \\ \langle \mathcal{I}(\delta B)^2 \rangle &= -2\pi^2 \int \frac{dq}{q} P_B(q) \frac{D}{q} : \end{aligned}$$

one can write the convolution part as either something proportional to one or the other. In any case, the two limits differ only by a factor of 2/3, so we can take either one: the mistake we make is at most this much. Physically, the first option might be more justified, that is, turbulence in electron density extends beyond, at larger scales, that for the magnetic field, so, for concreteness, we choose this in what follows. The main result then reads

$$\langle \mathcal{I}(\delta n \delta B)^2 \rangle = -\frac{8\pi}{3} \langle \mathcal{I}(\delta B)^2 \rangle \int \frac{dp}{p} P_n(p).$$

As this relation illustrates, everything can be predicted with the mild assumption that we know the features of the electron density spectrum, and there is no necessity to specify the properties of the magnetic field random fluctuations. Notice that thus far the only approximation we have employed is that the IR dominates the fluctuation spectra.

Results

We need to know the average electron density $\langle n \rangle$ and regular magnetic field $\langle B \rangle$, and the spectrum of the electron density fluctuations $P_n(q)$, in order to be able to extract the deflections from the RM data bypassing the magnetic field fluctuations.

The spectrum P_n can be written as

$$\langle \delta n^2 \rangle(\bar{r}) = \int d^3 q \frac{C_n^2 e^{-i\vec{r}\vec{q}}}{(q_0^2 + q^2)^{\alpha/2}},$$

where C_n^2 is the amplitude of a Kolmogorov spectrum for the electron density fluctuations, and the momentum IR cutoff is given by $q_0 = 2\pi/l_0$, with l_0 the largest scale of turbulence (with a given spectral index). This integral can be solved exactly, and it gives

$$\langle \delta n^2 \rangle(r) = \frac{2\pi^{3/2} C_n^2}{\Gamma(\alpha/2)} \left(\frac{r}{2q_0} \right)^{(\alpha-3)/2} K_{(\alpha-3)/2}(q_0 r).$$

These definitions enable us to compute all the terms in (17). As an example, following the results of Armstrong et al. (1995) and Haverkorn et al. (2008), for Kolmogorov electron density fluctuations ($\alpha = 11/3$), we find

$$\langle RM^2 \rangle \simeq c_1^2 \left\{ \langle n \rangle^2 + 3.1 C_n^2 l_0^{2/3} \right\} \langle \mathcal{I}^2(\delta B) \rangle + 1.1 C_n^2 D l_0^{5/3} \langle B \rangle^2,$$

which is the result (14) reported in the main text, and justifies the use of (6). The ensuing discussion then follows.

REFERENCES

- Ahn E.-J., Medina-Tanco G. A., Biermann P. L., Stanev T., 1999, *Phys.Rev.Lett.*
 Armstrong J., Rickett B., Spangler S., 1995, *Astrophys.J.*, 443, 209
 Beck R., 2001, *Space Sci. Rev.*, 99, 243
 Beck R., 2008, in F. A. Aharonian, W. Hofmann, & F. Rieger ed., *American Institute of Physics Conference Series Vol. 1085 of American Institute of Physics Conference Series, Galactic and Extragalactic Magnetic Fields.* pp 83–96
 Cordes J. M., Lazio T. J. W., 2002, *ArXiv Astrophysics e-prints*
 Gaensler B. M., Madsen G. J., Chatterjee S., Mao S. A., 2008, *PASA*, 25, 184
 Giacinti G., Kachelrieß M., Semikoz D. V., Sigl G., 2010, *JCAP*, 8, 36
 Golup G., Harari D., Mollerach S., Roulet E., 2009, *Astroparticle Physics*, 32, 269
 Górski K. M., Hivon E., Banday A. J., Wandelt B. D., Hansen F. K., Reinecke M., Bartelmann M., 2005, *ApJ*, 622, 759
 Harari D., Mollerach S., Roulet E., Sánchez F., 2002, *Journal of High Energy Physics*, 3, 45
 Harvey-Smith L., Madsen G. J., Gaensler B. M., 2011, *Astrophys.J.*, 736, 83
 Haverkorn M., Brown J., Gaensler B., McClure-Griffiths N., 2008
 Jansson R., Farrar G. R., 2012
 Kronberg P. P., 1994, *Rept.Prog.Phys.*, 57, 325
 Lyne A. G., Manchester R. N., Taylor J. H., 1985, *MNRAS*, 213, 613
 Prouza M., Šmída R., 2003, *A&A*, 410, 1
 Pshirkov M. S., Tinyakov P. G., Kronberg P. P., Newton-McGee K. J., 2011, *ApJ*, 738, 192
 Regis M., 2011, *Astropart.Phys.*, 35, 170
 Savage B. D., Wakker B., 2009, *Astrophys.J.*, 702, 1472
 Schnitzeler D., 2012
 Schnitzeler D. H. F. M., 2010, *MNRAS*, 409, L99
 Stanev T., 1997, *ApJ*, 479, 290
 Takami H., Sato K., 2008, *ApJ*, 681, 1279

Taylor A. R., Stil J. M., Sunstrum C., 2009, ApJ, 702, 1230

Taylor J., Cordes J., 1993, Astrophys.J., 411, 674

Tinyakov P. G., Tkachev I. I., 2002, Astroparticle Physics,
18, 165

Tinyakov P. G., Tkachev I. I., 2005, Astroparticle Physics,
24, 32